Available online at www.sciencedirect.com
ScienceDirect
International Journal of Pharmaceutics 350 (2008) 351–360
INTERNATIONAL JOURNAL OF PHARMACEUTICS
www.elsevier.com/locate/ijpharm

Pharmaceutical Nanotechnology

Microemulsions containing lecithin and sugar-based surfactants: Nanoparticle templates for delivery of proteins and peptides

Anja Graf [a,*], Elisabeth Ablinger [b], Silvia Peters [a], Andreas Zimmer [b], Sarah Hook [a], Thomas Rades [a]

[a] *School of Pharmacy, University of Otago, Dunedin, New Zealand*
[b] *Institute of Pharmaceutical Sciences, Department of Pharmaceutical Technology, University of Graz, 8010 Graz, Austria*

Received 25 June 2007; received in revised form 10 August 2007; accepted 30 August 2007
Available online 5 September 2007

Abstract

Two pseudo-ternary systems comprising isopropyl myristate, soybean lecithin, water, ethanol and either decyl glucoside (DG) or capryl-caprylyl glucoside (CCG) as surfactant were investigated for their potential to form microemulsion templates to produce nanoparticles as drug delivery vehicles for proteins and peptides. All microemulsion and nanoparticle compounds used were pharmaceutically acceptable and biocompatible. Phase diagrams were established and characterized using polarizing light microscopy, viscosity, conductivity, electron microscopy, differential scanning calorimetry and self-diffusion NMR. An area in the phase diagrams containing optically isotropic, monophasic systems was designated as the microemulsion region and systems therein identified as solution-type microemulsions. Poly(alkylcyanoacrylate) nanoparticles prepared by interfacial polymerisation from selected microemulsions ranged from 145 to 660 nm in size with a unimodal size distribution depending on the type of monomer (ethyl (2) or butyl (2) cyanoacrylate) and microemulsion template. Generally larger nanoparticles were formed by butyl (2) cyanoacrylate. Insulin was added as a model protein and did not alter the physicochemical behaviour of the microemulsions or the morphology of the nanoparticles. However, insulin-loaded nanoparticles in the CCG containing system decreased in size when using butyl (2) cyanoacrylate. This study shows that microemulsions containing sugar-based surfactants are suitable formulation templates for the formation of nanoparticles to deliver peptides.

Keywords: Microemulsions; Nanoparticles; Alkylcyanoacrylate; Self-diffusion NMR; Protein delivery; Insulin

1. Introduction

With the rapid advances in genetics and proteomics, an increasing number of peptide and protein therapeutics are being developed. This has provided formulation scientists with a new challenge as these molecules are highly susceptible to enzymatic degradation in the gastrointestinal tract and have inherently poor absorption properties. However, novel controlled delivery systems for protein and peptide drugs that can overcome absorption and enzymatic barriers may result in an alternative safe and effective oral delivery strategy, hence increasing patient compliance and successful therapy.

Since poly(alkylcyanoacrylate) (PACA) nanoparticles emerged as a new class of particulate drug delivery systems in the 1980s, numerous studies have been undertaken to exploit their potential for biomedical and pharmaceutical applications (Vauthier et al., 2003). PACA nanoparticles have gained extensive interest and are considered amongst the most promising polymer based colloidal drug delivery systems for controlled and targeted drug delivery (Vauthier et al., 2003). This is due to their biocompatibility and biodegradability (Couvreur et al., 1986, 1996), the simple manufacturing process, the potential for scaling-up (Al Khouri et al., 1986; Allemann et al., 1993), their ability to efficiently entrap proteins (Watnasirichaikul et al., 2000; Pitaksuteepong et al., 2002) and to provide protection from enzymatic degradation (Lowe and Temple, 1994), and their ability to facilitate the absorption of peptides from the gut lumen (Damge et al., 1987).

Not only have PACA nanoparticles been reported to possess the required qualities for efficient delivery of proteins and peptides but also the microemulsions used to make them have been shown to improve the oral absorption of peptides (Sarciaux et

* Corresponding author. Tel.: +64 3 479 3984; fax: +64 3 479 7034.
E-mail address: anja.graf@stonebow.otago.ac.nz (A. Graf).

0378-5173/$ – see front matter © 2007 Elsevier B.V. All rights reserved.
doi:10.1016/j.ijpharm.2007.08.053

al., 1995; Watnasirichaikul et al., 2002b). Microemulsions are dispersed systems of water, oil and a surfactant/cosurfactant mixture. Importantly, from a formulation viewpoint, they form spontaneously and are thermodynamically stable (Lindman and Stilbs, 1987; Moulik and Paul, 1998). Microemulsions have complex and diverse microstructures varying from droplet-to bicontinuous- and solution-types (Lindman and Stilbs, 1987). Solution-type microemulsions are reported to be molecular dispersions of all components (Lindman and Stilbs, 1987). PACA nanoparticle preparation by interfacial polymerisation of microemulsions was first introduced by Gasco and Trotta (Gasco and Trotta, 1986) using a water-in-oil (w/o) microemulsion. Watnasirichaikul et al. developed a simple one-step process using ethylcyanoacrylate as a monomer and a w/o-droplet-type microemulsion (Watnasirichaikul et al., 2000). Concerns about the toxicity of cyanoacrylates with shorter side chains (Gipps et al., 1987; Lherm et al., 1992) have led to the use of butyl (2) cyanoacrylate as a suitable monomer in addition to ethyl (2) cyanoacrylate in microemulsion polymerisation. Butyl (2) cyanoacrylate is one of the two monomers that have been approved by the FDA as tissue adhesives in human use (Singer et al., 2004). The use of microemulsions as templates for polymeric nanoparticles is not limited to water-in-oil microemulsions. Krauel et al. have demonstrated that all types of microemulsions including water-free microemulsions (Krauel et al., 2005, 2006) can be used as templates to form PACA nanoparticles. Moreover, using biocompatible microemulsions as nanoparticle templates has the advantage of being able to omit the separation step of the particles from the template after polymerisation and this in turn enables the simple one-step formulation of delivery systems combining the benefits of both microemulsions and nanoparticles for the delivery of proteins and peptides. In fact, Watnasirichaikul et al. have investigated this combination strategy of nanoparticles dispersed in a w/o microemulsion and found it to be beneficial for the intragastric delivery of insulin to diabetic rats (Watnasirichaikul et al., 2002b).

Microemulsion excipients in the current study were chosen with respect to biocompatibility and biodegradability. Isopropyl myristate is a non-toxic ester with good systemic and local tolerance (Fiedler, 2002) and is pharmaceutically acceptable as the oil component in microemulsions (Aboofazeli and Lawrence, 1993). In recent years sugar-based surfactants, alkylpolyglucosides, have emerged as a novel, important class of natural surfactants with excellent biodegradability and good skin tolerance. Alkylpolyglucosides are known to form lamellar liquid crystalline phases which transform to microemulsions in the presence of cosolvents (Fiedler, 2002; Savic et al., 2006). They represent a class of biodegradable surfactants that may be beneficial as alternatives to other non-ionic surfactants to form microemulsions in combination with cosurfactants (Fukuda et al., 2001). Lecithin is an integral part of cell membranes and thus highly biocompatible. It is widely used as an emulsifier for food products, cosmetics and in pharmaceutical systemic applications such as total parenteral nutrition and for the preparation of liposomes (Fiedler, 2002). Lecithin has also been studied for its absorption-enhancing properties in an intranasal insulin formulation (Anonymous, 1991). Due to its molecular structure, soybean lecithin tends to form lamellar liquid crystals in aqueous dispersions but it has been reported to form microemulsions in combination with short-chain alcohols such as ethanol, thereby making it suitable for oral drug delivery (Aboofazeli and Lawrence, 1993; Saintruth et al., 1995; Trotta et al., 1996, 1999).

The aims of this study were to establish and characterise a biocompatible microemulsion-system using lecithin and sugar-based surfactants, to identify the types of microemulsions formed and to explore their potential as nanoparticulate carriers for the delivery of bioactives by interfacial polymerisation of the microemulsion template with alkylcyanoacrylates. Using microemulsions with different microstructure and different aqueous fractions offers the advantage of having large and variable formulation options for solubilizing proteins and peptides.

2. Materials and methods

2.1. Materials

Isopropyl myristate (IPM) was purchased from Sigma (St. Louis, MO, USA). Soybean lecithin (Epikuron 200) was supplied by Degussa Texturant Systems (Hamburg, Germany). Decyl glucoside (DG, Oramix NS 10) and capryl-caprylyl glucoside (CCG, Oramix CG 110) were a gift from Seppic (Paris, France). Ethanol was supplied by AnchorEthanol (Auckland, New Zealand). The monomers ethyl (2) cyanoacrylate (Sicomet 40) and butyl (2) cyanoacrylate (Sicomet 6000) were donated by Henkel Loctite (Hannover, Germany). Chloroform was obtained from Merck (Darmstadt, Germany) and human insulin (Humulin R, 100 IU/ml) was purchased from Eli Lilly Ltd. (Auckland, New Zealand). Distilled water was used throughout the experiments.

2.2. Methods

2.2.1. Preparation and characterisation of microemulsions, construction of phase diagram

Samples were prepared by mixing appropriate amounts of IPM, water and surfactant/cosurfactant mixture in vials by shaking. The surfactant/cosurfactant mixture was prepared at a ratio of 32.6% lecithin to 40.4% DC or CCG to 27% ethanol (w/w) (Trotta et al., 2003). All sample preparations were carried out at room temperature. The pseudo-ternary phase diagrams were constructed by preparing samples at 66 compositions within the phase diagram for an overview of the phase behaviour of the different systems. Determination of the boundaries of the microemulsion region was then refined by a titration process of homogeneous mixtures of IPM, surfactant and cosurfactant, with water. For the titration process water was added dropwise to an IPM/surfactant blend with a varying ratio of IPM to surfactant-mix ranging from 9:1 to 1:9 (w/w). Samples were left for equilibration between each addition of water for 10 min and were visually examined for transparency. Microemulsion samples with a surfactant-to-water ratio of 9:1 (w/w) were prepared for further characterisation. For microemulsions containing insulin, the aqueous component was replaced by Humulin R.

2.2.1.1. Polarizing light microscopy. Samples initially prepared for the construction of the phase diagram as well as the microemulsion samples prepared for detailed studies of the microemulsion phase boundary were inspected with a polarizing light microscope (Nikon Optiphot PFX, Tokyo, Japan) to identify microemulsions (non-birefringent) and liquid crystalline structures (birefringent). A digital camera (Nikon CoolPix 990, Japan) was attached to the microscope for capturing images of the different structures.

2.2.1.2. Viscosity. Viscosity of the systems was measured using a Brookfield DVIII rheometer (Brookfield Engineering Laboratories, Stroughton, MA) fitted with a CP-42 cone spindle. Brookfield Rheocalc operating software was used to control the measurement. A sample volume of 1 ml was used. The measurements were performed in triplicate at 25 °C.

2.2.1.3. Conductivity. Conductivity measurements were carried out for the microemulsion samples using a Riac CM/100 conductivity meter fitted with an YSI 3481 electrode having a cell constant of 0.11 cm^{-1} (Yellow Springs Instruments Inc., Yellow Springs, OH). Electrical conductivity was measured of microemulsions without addition of salt and additionally of microemulsions where the aqueous phase had been replaced by a 1 mM sodium chloride solution. Incorporation of 1 mM sodium chloride did not affect the phase behaviour of the systems investigated. Measurements were carried out in triplicate at 25 °C.

2.2.1.4. Cryo-field emission scanning electron microscopy (cryo-FESEM). Microemulsions were loaded into copper rivets and plunge frozen in liquid propane at a temperature of −180 °C with a Reichert KF 80 cryofixation system (Leica, Wetzlar, Germany). Samples were stored in liquid nitrogen before being transferred into the cryo-stage (Gatan, Alto 2500, UK) of the microscope (JEOL, JSM-6700F, Japan). After fracturing the sample with a knife it was viewed at a temperature of −140 °C and an accelerating voltage of 2.5 kV.

2.2.1.5. Differential scanning calorimetry (DSC). DSC measurements were performed with a DSC TA Q100 instrument equipped with a refrigerated cooling system (TA Instruments, New Castle, DE). Nitrogen with a flow rate of 50 ml/min was used as purge gas. Approximately 6–11 mg of sample was weighed precisely into hermetically sealable aluminium pans. An empty hermetically sealed pan was used as reference. Measurements were carried out in a cooling mode cooling the sample down from 25 to −50 °C at a cooling rate of 5 °C/min. Sample thermograms were analysed using the TA Universal Analysis software 4.0 C.

2.2.1.6. Self-diffusion NMR. Self-diffusion NMR experiments were performed applying a FT-PGSE (Fourier transform-pulse gradient spin echo) sequence on a Varian Inova (500 MHz) NMR instrument equipped with Performa II-Z gradient coils (Varian, Palo Alto, CA) at a constant temperature of 25 °C. Three millimetre diameter NMR sample tubes (Wilmad-Labglass, Buena, NJ) were used with a sealed capillary of 2.2-Dimethyl-2-silapentane-5-sulfonate sodium salt (DSS) dissolved in D_20 as internal reference. ^{1}H NMR spectra of the neat components and microemulsions were acquired and compared to obtain characteristic peak shifts for each component for analysis. A total of 17 echoes were acquired over an increasing range of the gradient amplitude from 0 to 0.426 T m^{-1} keeping the length of the z-gradient pulse constant. The gradient pulse length (δ) and diffusion time (Δ) were experimentally adjusted to slow ($\delta = 5$ ms, $\Delta = 200$ ms), medium ($\delta = 2.5$ ms, $\Delta = 100$ ms) or fast ($\delta = 1$ ms, $\Delta = 100$ ms) diffusing species. Analysis was performed with Sigmaplot 9.0 software using the Stejskal–Tanner equation:

$$\frac{I}{I_0} = \exp\left[-D(\gamma\delta g)^2\left(\Delta - \frac{\delta}{3}\right)\right] \quad (1)$$

The diffusion coefficients (D) were obtained from an exponential curve fit to eq. (1) where I is the signal intensity at gradient strength g and I_0 the signal intensity when no gradient is applied, γ is the gyromagnetic ratio of ^{1}H, δ is the pulse duration and Δ diffusion time between the gradient pulses.

2.2.2. Preparation and characterisation of nanoparticles

2.2.2.1. Preparation of nanoparticles. Nanoparticle preparation by interfacial polymerisation was based on the method of Watnasirichaikul et al. (Watnasirichaikul et al., 2002a). Briefly, 200 mg of either ethyl (2) cyanoacrylate or butyl (2) cyanoacrylate were dissolved in 600 mg chloroform. This solution was slowly added to 10 g of the selected microemulsion template. The sample was continuously stirred at 700 rpm overnight at 4 °C using a magnetic bar.

2.2.2.2. Characterisation of nanoparticles. Particle size, size distribution and polydispersity index were measured using photon correlation spectroscopy (PCS). The zetapotential of the nanoparticles dispersed in a 1 mM sodium chloride solution was determined by electrophoretic mobility (Zetasizer Nano ZS, Malvern Instruments Ltd., UK). The morphology of the particles was studied by scanning electron microscopy at an accelerating voltage of 10 kV (JEOL, JSM-6700F, Japan) after sputter-coating with gold and palladium. Particles were separated from the microemulsion template after polymerisation by centrifugation at 51,500 × g for 1 h followed by repeated washing in ethanol and centrifugation at 18,500 × g for 10 min at 25 °C (Beckman J2/MC Centrifuge, JA20.1 rotor). The resulting nanoparticle pellet was redispersed in ethanol and further diluted with ethanol containing 0.2% (w/w) Tween 80 for size measurements to prevent aggregation. The ethanol dispersion was placed on the sample holder, and the ethanol was allowed to evaporate before sputter-coating.

2.2.2.3. Determination of entrapment efficiency of insulin. Entrapment efficiency (EE) of insulin in PACA nanoparticles was determined based on the method of McDowell (McDowell, 2005). Briefly, 0.5 g of a polymerised insulin-loaded microemulsion was diluted with 3 ml MilliQ water (adjusted to pH 2.5 with hydrochloric acid). 600 μl of the obtained dispersion was mixed with 600 μl of 80% (v/v) methanol in water (pH 2.5).

Subsequently, nanoparticles, residual oil and surfactant were isolated from the hydro-methanolic phase by centrifugation (Eppendorf 5417C centrifuge) at 12,000 × *g* for 12 min at 25 °C. The concentration of insulin in the hydro-methanolic phase was quantitatively measured by HPLC with an assay adapted from Watnasirichaikul et al. (Watnasirichaikul et al., 2000) using an Agilent 1200 Series instrument (Agilent Technologies, Waldbronn, Germany). Briefly, a reverse phase column (Jupiter 5 μ C18 300A, 250 × 4.60 mm, Phenomenex) was kept constant at 50 °C. The flow rate of the mobile phase (23.5% (w/w) acetonitrile in MilliQ water) was maintained at 1.4 ml/min. A 50 μl sample was automatically injected and monitored at a wavelength of 212 nm. Data was collected, integrated and analysed using the Agilent Technologies software. The amount of entrapped insulin was calculated by subtracting the detected insulin concentration in the supernatant of a polymerised microemulsion from the insulin concentration of an unpolymerised microemulsion with known amount of insulin.

3. Results and discussion

3.1. Characterisation of microemulsions

The phase diagrams of the pseudo-ternary systems isopropyl myristate/soybean lecithin/ethanol/water and either DG or CCG are shown in Fig. 1. Areas of the phase diagram containing one-phase systems were identified and samples therein characterised as microemulsions. Adjacent to the microemulsion region a lamellar liquid-crystalline gel region was found. This was confirmed by polarising light microscopy where lamellar liquid-crystalline structures, such as maltese crosses and oily streaks were seen. When the aqueous component of the microemulsion was replaced by insulin, no change in phase behaviour of the system was evident. This could be due to a stabilizing effect from the sugar-based surfactants as it has been reported that once formation of a microemulsion has been achieved using alkylpolyglucosides neither temperature nor electrolyte additives have a strong influence on the microemulsion stability. This finding was confirmed using conductivity measurements (see Section 3.1.1). The phase behaviour of both systems was found to be very similar despite the use of two different sugar-based surfactants. DG is a monomeric C_{10} (C = carbon chain length) glucoside and CCG is an oligomeric $C_{8\text{-}10}$ glucoside. However, the complexity of these naturally derived compounds and thus a multi-factorial influence on their phase behaviour has been reported (von Rybinski and Hill, 1998; Boyd et al., 2000). It is a function of not only their alkyl chain length but also the degree of polymerisation and anomeric purity. Hence without further detailed studies on the composition of the surfactants it is difficult to conclude from structural differences in the molecule to the phase behaviour of the two surfactants used in this study.

3.1.1. Viscosity and conductivity

Viscosity and conductivity measurements exhibited a continuously increasing trend with increasing water fraction (Fig. 2).

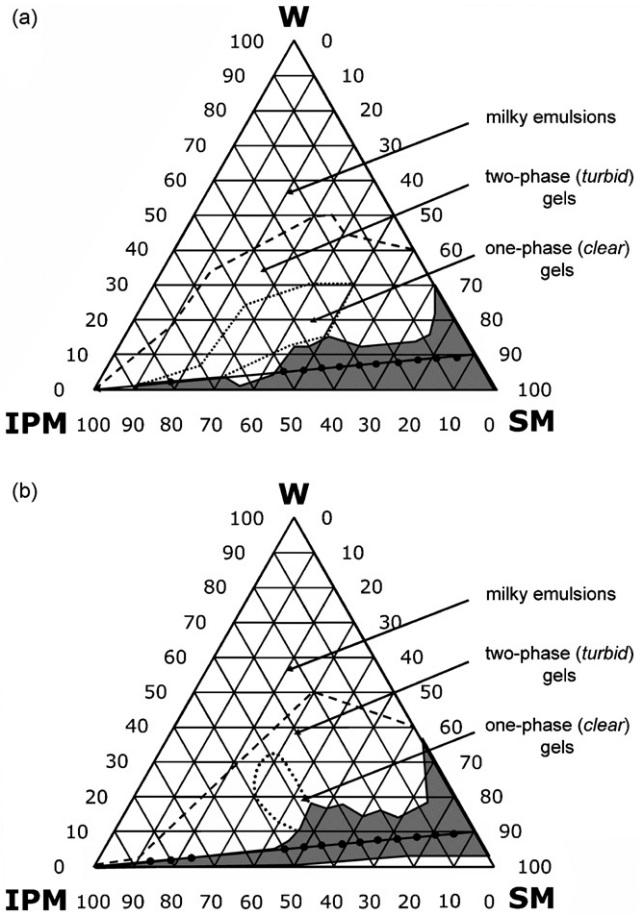

Fig. 1. Pseudo-ternary phase diagrams of isopropyl myristate (IPM), surfactant-mix (SM) and water (W) with microemulsion (ME) areas (shaded). Samples at a constant surfactant-to-water ratio of 9:1 (w/w) (line in shaded area) were chosen for further investigations ((●) solution-type microemulsions). Gels represent liquid-crystalline structures. (a) DG containing microemulsion-system, (b) CCG containing microemulsion-system.

The increase in viscosity for the microemulsions is likely due to an increasing amount of the surfactant-mix rather than an increasing number of water droplets, typical for a w/o droplet microemulsion (Krauel et al., 2005), as this would not correlate with the high conductivity of the samples (see below). No critical concentrations, indicative of a change in microemulsion type could be identified.

Conductivity >1 μS/cm has been reported to be indicative of bicontinuous or solution-type microemulsions (Krauel et al., 2005). Measurable conductivity even at low water concentrations is not surprising for solution-type microemulsions. An increase in conductivity was also found by Alany et al. for the ethyl oleate/sorbitan monolaurate-polyoxyethylene 20 sorbitan mono-oleate/butanol/water microemulsion system due to a progressive head group hydration of the surfactant creating a conductive entity (Alany et al., 2001).

For the DG containing system, samples with 55–75% and 85–95% oil concentration and with 55–70% and 90–95% oil concentration for the CCG containing system have not been included in viscosity and conductivity measurements due to their birefringent (liquid-crystalline) nature.

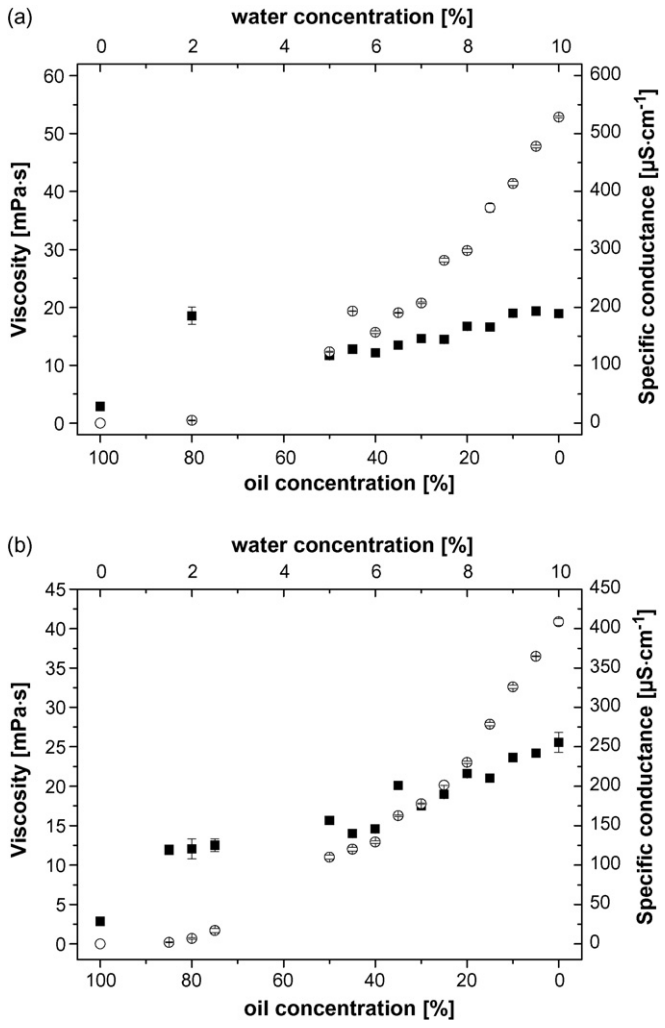

Fig. 2. Viscosity (■) and conductivity (◯) of microemulsions at a constant surfactant-to-water ratio of 9:1 (w/w) in comparison to isopropyl myristate (100% oil concentration) and water. Values represent mean ± standard deviation, $n = 3$. (a) DG containing microemulsion-system and (b) CCG containing microemulsion-system.

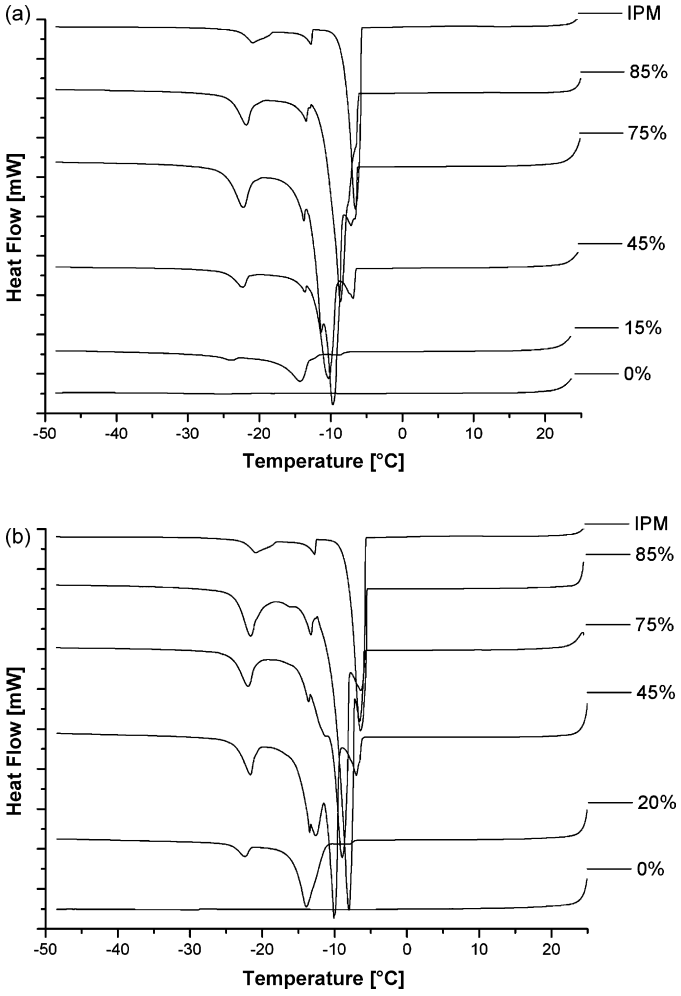

Fig. 3. Differential scanning thermograms of microemulsions at a constant surfactant-to-water ratio of 9:1 (w/w) upon decreasing amount of oil (100% (IPM), 85%, 75%, 45%, 20%, 15%, 0% oil). (a) DG containing microemulsion-system and (b) CCG containing microemulsion-system.

The DG sample at 80% oil concentration (Fig. 2a)) revealed a non-Newtonian flow behaviour indicative of liquid-crystalline structures (Alany et al., 2001). This is due to its position in the phase diagram proximately located at the liquid-crystalline gel region and its immediate transformation to a liquid crystal upon ethanol evaporation.

3.1.2. Differential scanning calorimetry (DSC)

The DSC thermograms (Fig. 3) did not reveal any water crystallization exotherm upon cooling to −50 °C for the DG and CCG containing microemulsions. This is likely to be due to the very low water concentration in the microemulsion systems. However, the absence of any water freezing peak in the binary water-surfactant mixtures indicates presence of a strong water-surfactant interaction (Garti et al., 1996). This also proves the absence of phase separation which can be a problem associated with sub-zero temperature DSC as the cooling rate in some cases is not fast enough to retain the microstructure of the microemulsion (Garti et al., 2000). The water in the systems investigated in this study is likely to be bound by head group hydration of the surfactant. The surfactant has to be saturated with water before a (free) water freezing peak can be observed (Garti et al., 2000). In combination with the viscosity and conductivity data this behaviour suggests molecularly dispersed systems and thus solution-type microemulsions. Furthermore, a shift of the endothermic IPM freezing peaks to lower temperatures as seen in the thermograms could result from the interaction of oil with the surfactant or simply represent a depression of freezing point due to an increase in the entropy of mixing.

3.1.3. Cryo-FESEM

Structural investigations carried out by cryo-FESEM revealed three different morphological domains within the microemulsion samples at a surfactant-to-water ratio of 9:1 (w/w) upon increasing oil concentration (Fig. 4). The surfactant dominates the structural appearance up to an oil concentration of 50% (Fig. 4d). Lamellar structures were found between 50 and 70% oil (Fig. 4c) changing to an appearance dominated by

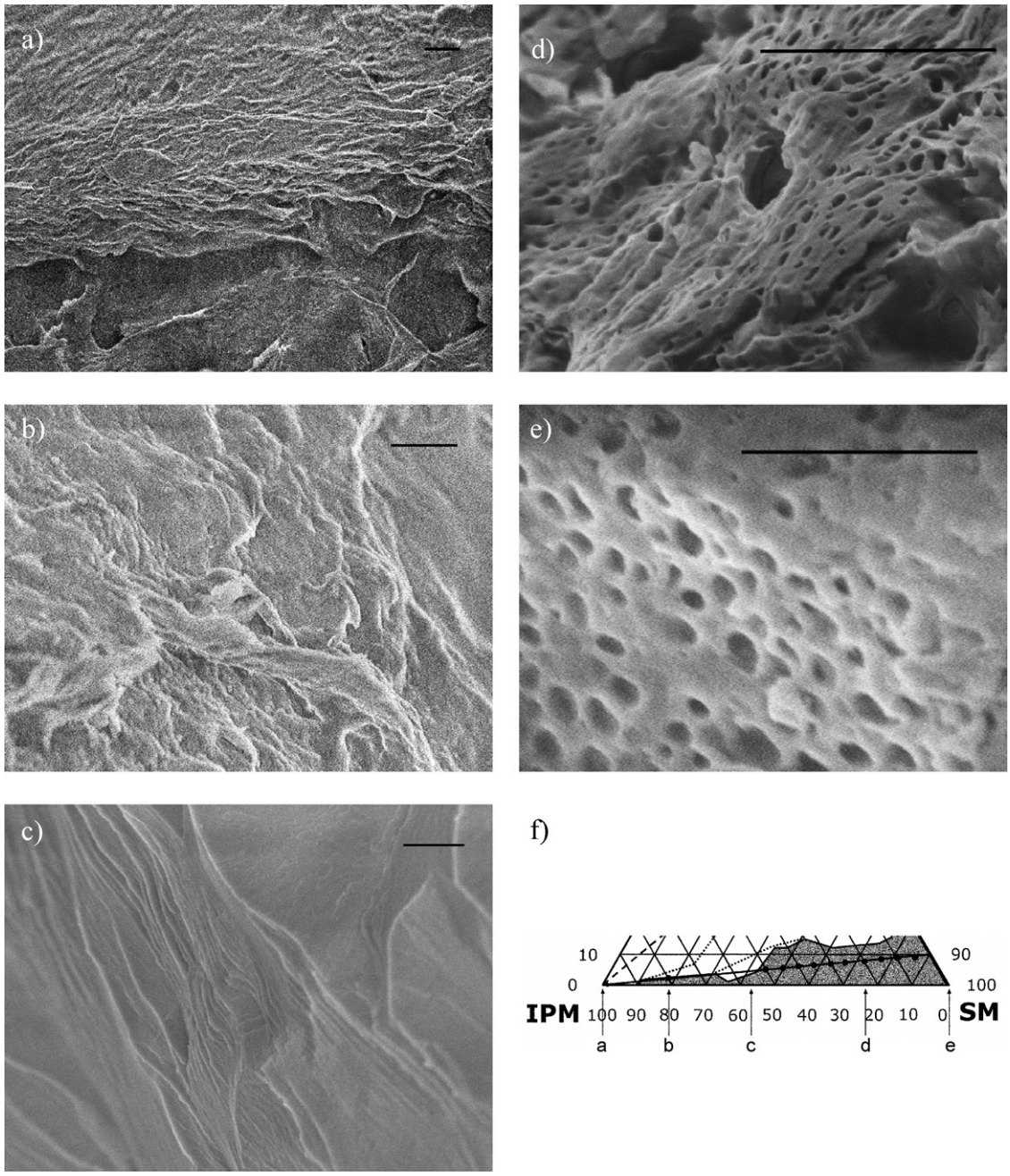

Fig. 4. Cryo-field emission scanning electron micrographs of selected samples from the DG containing system at a surfactant-to-water ratio of 9:1 (w/w) and pure oil and pure surfactant-mix (SM) with (a) 100% IPM (pure oil, IPM), (b) 80% IPM (oil-dominated), (c) 55% IPM (lamellar structures), (d) 20% IPM (surfactant-dominated) and (e) 0% IPM/100% SM (pure surfactant-mix), as indicated by arrows in the cut-out of the phase diagram (f). Bar represents 1 μm.

the oil from concentrations ≥70% oil onwards (Fig. 4b). Unlike other studies (Krauel et al., 2005; Boonme et al., 2006a,b) the difference in the morphology as seen in the micrographs did not specifically relate to the microemulsions structure (which always was of the solution type). It is remarkable that the differences found rather result from the dominating compound in the respective sample and as such reveal the molecularly dispersed solution-type nature of these microemulsions. The micrographs shown are from the DG containing system but are representative of both systems.

3.1.4. Self-diffusion NMR

Self-diffusion NMR measurements were carried out for the DG containing microemulsion-system. The instrument was calibrated with water resulting in a diffusion coefficient for water of $2.28 \times 10^{-9}\ m^2\ s^{-1}$ which is in excellent agreement with the literature (Ghi et al., 2002). Characteristic peaks for each component chosen for analysis are shown in Fig. 5. Identification of the microemulsion type can be achieved by comparing the self-diffusion coefficients of the individual components with those measured for the pure components. The dispersed

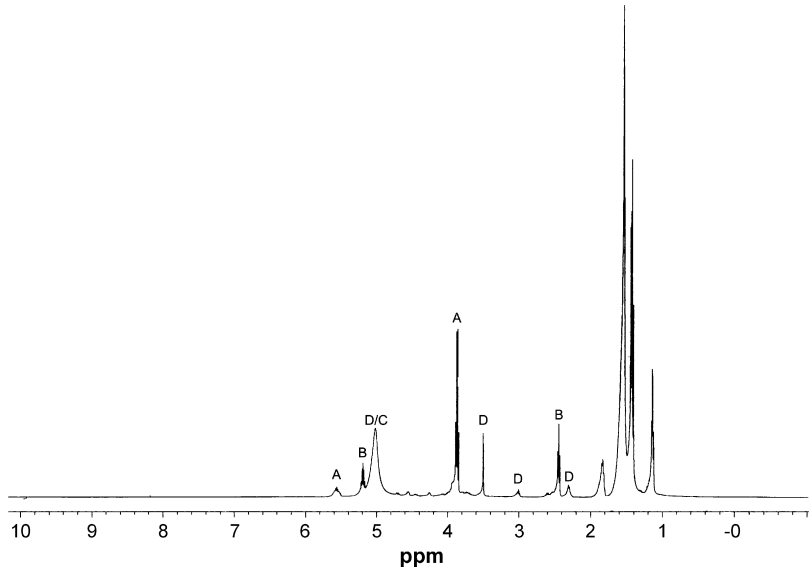

Fig. 5. ^{1}H NMR spectrum of a DG containing microemulsion sample indicating characteristic peaks of the components used for the determination of diffusion coefficients. A: ethanol as part of the surfactant-mix, B: oil, C: water associated with surfactant-mix, D: lecithin and DG as part of the surfactant-mix.

droplet components will diffuse more slowly than the continuous phase components when droplet-type microemulsions are formed, and in case of bicontinuous or solution-type microemulsions the individual components diffuse rapidly (Lindman et al., 1981). Diffusion of the individual components was analysed using at least two characteristic peaks which belong to different structures within the molecule and could be deconvoluted from overlapping peaks during analysis. However, not all of these peaks could be integrated over the entire range of samples.

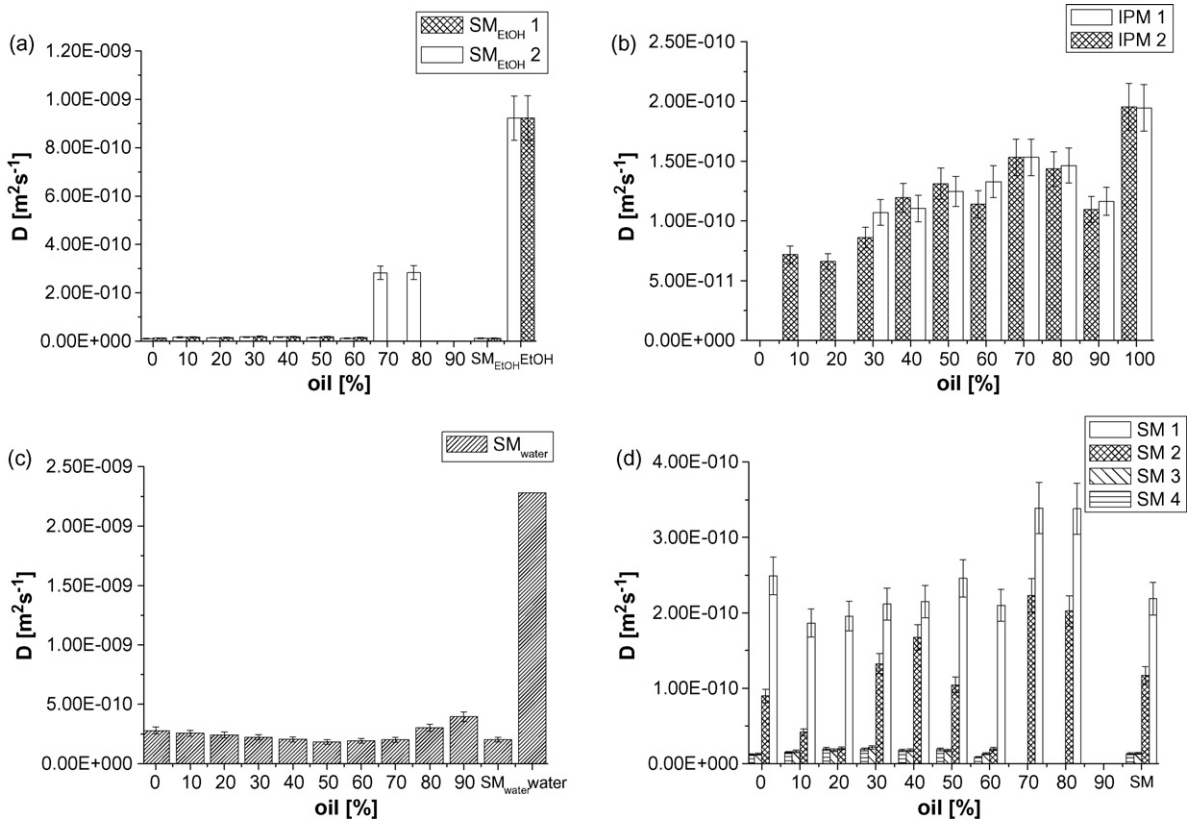

Fig. 6. Self-diffusion coefficients of microemulsion components with varying oil content for DG containing systems at a constant surfactant-to-water ratio of 9:1 (w/w). (a) Ethanol associated with the surfactant-mix (SM_{EtOH}) compared to pure ethanol, (b) oil (IPM), (c) water associated with the surfactant-mix (SM_{water}) compared to pure surfactant-mix (SM) and pure water, respectively, (d) lecithin and DG within the surfactant-mix (SM). Individual bars represent characteristic peaks which belong to different structures within the molecule.

Diffusion of the cosurfactant ethanol was significantly different to pure ethanol due to its association with the surfactant-mix but did not change for the microemulsion samples. A change in ethanol diffusion was only found in the liquid crystal containing samples (Fig. 6a). This is due to their lamellar arrangement in which ethanol can diffuse along the hydrophilic layer. Diffusion of IPM was found to be decreasing slightly with decreasing oil concentration (Fig. 6b). This in turn is related to an increase in surfactant concentration and thus an increase in viscosity causing the diffusion of IPM to be slowed down. The comparison of diffusion of pure water to diffusion of water in these systems clearly revealed a strong association of water with the surfactant (Fig. 6c). Water diffuses as fast as the surfactant-mix except in the sample containing 90% oil which in fact is outside the microemulsion region, and the liquid crystal containing sample (80% oil) where water again can diffuse faster along the lamellae of the liquid crystals. Water diffusing at the same rate as the surfactant-mix could indicate a w/o-droplet type system. In this case one would also expect the surfactant-mix to be slowed down from its pure state due to localisation around the droplets. This, however, could not be seen in the diffusion of the surfactant-mix (Fig. 6d). Instead the surfactant-mix in the samples diffuses at the same rate as in its neat state with the exception of the liquid crystal containing samples where the diffusion coefficient is increased. Faster self-diffusion of the surfactant in the systems studied results from eliminating the retardation of the surfactant by self-association in its neat state (Nilsson and Lindman, 1982). Taken together, these finding indicate the formation of solution-type microemulsions. From our NMR results we conclude the following: ethanol being highly miscible with both water and surfactant cannot be assumed mainly to be located at the interphase (Lindman et al., 1981). Further, no separate water domain is formed for ethanol to diffuse into because of water being taken up by head group hydration. Hence ethanol stays bound to the surfactant and diffuses at the same rate whereas in lamellar liquid crystal containing sample (sample with 70 and 80% oil concentration, respectively) ethanol can diffuse into the water layers due to the distinct orientation of polar heads of the surfactant resulting in an increase in ethanol diffusion. The slight retardation effect in oil diffusion can be explained taking into account the increase in viscosity with increasing surfactant fraction. Water diffusion clearly follows the diffusion of the surfactants confirming the results from conductivity and DSC measurements, that is the binding of water by head group hydration of the surfactant.

3.2. Characterisation of nanoparticles

Polymerisation with butyl (2) cyanoacrylate as monomer resulted in larger particles than polymerisation with ethyl (2) cyanoacrylate (Table 1). Depending on the microemulsion template, the size ranged from 145 to 180 nm for ethyl (2) cyanoacrylate and from 215 to 660 nm for butyl (2) cyanoacrylate. The reason for these findings is likely to be the lower polymerisation rate of butyl (2) cyanoacrylate as compared to ethyl (2) cyanoacrylate (Sharma et al., 2003). Size did not change for unloaded and insulin-loaded poly(ethylcyanoacrylate) nanoparticles. Poly(butylcyanoacrylate) nanoparticles loaded with insulin however, were significantly smaller in size than their empty counterparts for microemulsions containing CCG but not for microemulsions containing DG. This may indicate that insulin is involved in the polymerisation process (Watnasirichaikul et al., 2000), and has a greater influence on the more slowly polymerising monomer butyl (2) cyanoacrylate. The reason for this phenomenon only being evident in the CCG containing system and not in the DG containing system is currently unclear. Moreover, it was not possible to satisfactorily polymerise the CCG sample containing 20% of oil with ethyl (2) cyanoacrylate due to a gelation occurring during the polymerisation process.

Particles usually appeared spherical but aggregated under the SEM (Fig. 7) and were smaller in size than in the PCS measure-

Table 1
Size, polydispersity index (PdI), zetapotential and entrapment efficiency (EE) for unloaded and insulin-loaded poly(ethylcyanoacrylate) (E) and poly(butylcyanoacrylate) (B) nanoparticles prepared by interfacial polymerisation of solution-type microemulsions with 80% (80), 50% (50) and 20% (20) oil concentration

unloaded Sample	Size (nm)	PdI	Zeta (mV)	Insulin (I)-loaded sample	Size (nm)	PdI	Zeta (mV)	EE (%)
(a)								
80-E	147 ± 3	0.110 ± 0.011	−23.6 ± 1.8	I-80-E	156 ± 4	0.109 ± 0.010	−27.6 ± 2.9	11.3 ± 0.6
50-E	171 ± 2	0.171 ± 0.022	−25.7 ± 1.7	I-50-E	180 ± 7	0.112 ± 0.017	−26.3 ± 5.5	17.9 ± 3.5
20-E	177 ± 4	0.184 ± 0.013	−24.4 ± 9.7	I-20-E	179 ± 9	0.158 ± 0.022	−24.4 ± 3.8	14.5 ± 2.5
80-B	239 ± 19	0.156 ± 0.044	−45.5 ± 4.3	I-80-B	230 ± 12	0.142 ± 0.048	−56.3 ± 2.2	11.5 ± 0.5
50-B	261 ± 47	0.178 ± 0.032	−41.4 ± 8.9	I-50-B	367 ± 19	0.187 ± 0.012	−29.0 ± 2.1	13.3 ± 1.4
20-B	217 ± 11	0.139 ± 0.022	−25.7 ± 1.8	I-20-B	290 ± 58	0.120 ± 0.020	−36.0 ± 1.8	13.3 ± 1.7
(b)								
80-E	148 ± 4	0.155 ± 0.007	−21.5 ± 3.0	I-80-E	148 ± 9	0.147 ± 0.038	−24.2 ± 4.6	8.8 ± 3.3
50-E	159 ± 5	0.183 ± 0.004	−20.6 ± 3.6	I-50-E	161 ± 5	0.165 ± 0.015	−22.3 ± 2.1	12.6 ± 5.0
20-E	–	–	–	I-20-E	–	–	–	–
80-B	657 ± 75	0.125 ± 0.053	−35.6 ± 7.3	I-80-B	299 ± 51	0.157 ± 0.025	−41.8 ± 1.3	12.8 ± 4.3
50-B	424 ± 80	0.113 ± 0.031	−27.5 ± 3.2	I-50-B	261 ± 35	0.107 ± 0.025	−32.0 ± 3.1	13.9 ± 3.8
20-B	385 ± 50	0.084 ± 0.068	−27.8 ± 2.1	I-20-B	232 ± 20	0.132 ± 0.051	−37.4 ± 2.6	18.2 ± 2.4

(a) DG containing microemulsion-system and (b) CCG containing microemulsion-system. Values represent mean ± standard deviation, $n = 3$.

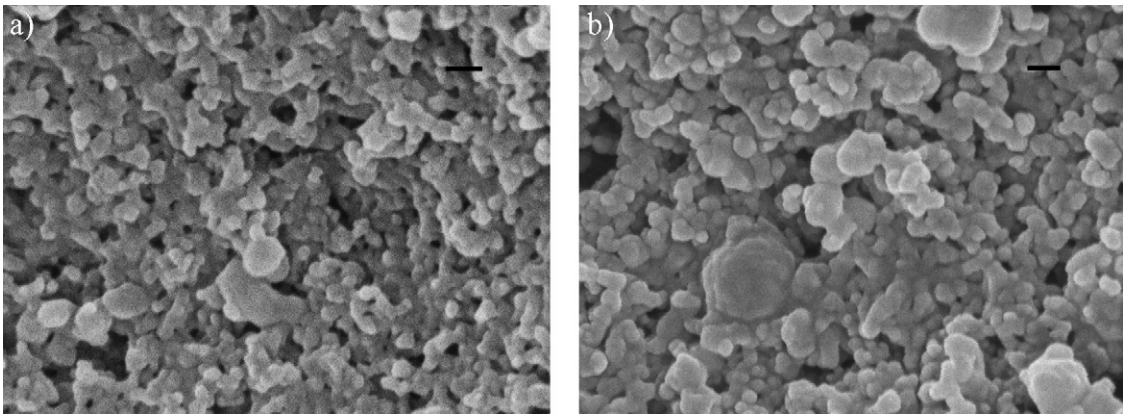

Fig. 7. Scanning electron micrographs of nanoparticles from selected microemulsions prepared by interfacial polymerisation ethyl (2) cyanoacrylate. (a) Nanoparticles from unloaded DG containing microemulsion (20% oil concentration), (b) nanoparticles from insulin-loaded DG containing microemulsion (20% oil concentration). Bar represents 100 nm.

ments for unloaded samples. This discrepancy between PCS and SEM data is due to hydration of the particles in solution when measured by PCS and/or shrinking of the particles during the drying step in the sample preparation for SEM (Bootz et al., 2004).

3.3. Entrapment of insulin

Entrapped insulin was determined indirectly by detecting the concentration of remaining insulin in the supernatant following an isolation process from the particles.

The entrapment efficiency of insulin in poly(ethyl-) and poly(butylcyanoacrylate) nanoparticles was in the range of 8.8–18.2% (Table 1). An explanation for this relatively low entrapment is that insulin is a relatively small molecule and is dissolved in the continuous water domains of these solution-type microemulsions and thus could easily escape the polymer network of the forming particle during the polymerisation process. This is in contrast to the situation in a droplet-type microemulsion where the molecule is confined within the droplet around which the polymerisation occurs and thus yields a higher entrapment (Watnasirichaikul et al., 2000; Krauel et al., 2005). The type of monomer can also influence the encapsulation process in that polycyanoacrylates with a longer alkyl chain result in a higher degree of interdigitation of the polymer (El-Samaligy et al., 1986) and thus might incorporate a higher amount of drug. However, in this study we found no consistent difference in entrapment efficiency between ethyl- and butylcyanoacrylate. This may be due to the lower polymerisation rate of butylcyanoacrylate (Sharma et al., 2003) in combination with the dynamics in a solution-type microemulsion as described above.

4. Conclusions

Pseudo-ternary systems containing lecithin and the sugar-based surfactants, decyl glucoside or capryl-caprylyl glucoside, *inter alia* form solution-type microemulsions. These can be used as nanoparticle templates for the incorporation of insulin using a one-step preparation method by interfacial polymerisation providing easy processing and scaling-up possibilities. Using self-diffusion NMR, it was possible to confirm on a molecular level dynamics that which can only be described on a bulk level with other techniques. Self-diffusion NMR has shown to give valuable insight into the complex structure of the pharmaceutically acceptable multi-component systems investigated in this study. PACA nanoparticles on the basis of lecithin and sugar-surfactant containing microemulsions are thus promising carriers for the delivery of bioactives.

Acknowledgements

The authors would like to thank the University of Otago for a scholarship for Anja Graf as well as the University of Graz and the federal state Oberösterreich, Austria for a scholarship for Elisabeth Ablinger. Thanks go to Henkel Loctite, Germany for donating the monomers. Further, we are thankful to SEPPIC, France and Degussa Texturant Systems, Germany for kindly supplying the surfactants used in this study. Liz Girvan is thanked for her assistance with electron microscopy techniques and Mervyn Thomas for assistance with NMR.

References

Aboofazeli, R., Lawrence, M.J., 1993. Investigations into the formation and characterization of phospholipid microemulsions. 1. Pseudo-ternary phase-diagrams of systems containing water-lecithin-alcohol-isopropyl myristate. Int. J. Pharm. 93, 161–175.

Alany, R.G., Tucker, I.G., Davies, N.M., Rades, T., 2001. Characterizing colloidal structures of pseudoternary phase diagrams formed by oil/water/amphiphile systems. Drug Dev. Ind. Pharm. 27, 31–38.

Al Khouri, F.N., Roblot-Treupel, L., Fessi, H., Devissaguet, J.P., Puisieux, F., 1986. Development of a new process for the manufacture of polyisobutylcyanoacrylate nanocapsules. Int. J. Pharm. 28, 125–132.

Allemann, E., Gurny, R., Doelker, E., 1993. Drug-loaded nanoparticles—preparation methods and drug targeting issues. Eur. J. Pharm. Biopharm. 39, 173–191.

Anonymous, 1991. Intranasal insulin formulation reported to be promising. Pharm. J. 17, 247.

Boonme, P., Krauel, K., Graf, A., Rades, T., Junyaprasert, V.B., 2006a. Characterisation of microstructures formed in isopropyl palmitate/water/Aerosol (R) OT: 1-butanol (2:1) system. Pharmazie 61, 927–932.

Boonme, P., Krauel, K., Graf, A., Rades, T., Junyaprasert, V.B., 2006b. Characterization of microemulsion structures in the pseudoternary phase diagram of isopropyl palmitate/water/Brij 97: 1-butanol. AAPS PharmSciTech 7, E1–E6.

Bootz, A., Vogel, V., Schubert, D., Kreuter, J., 2004. Comparison of scanning electron microscopy, dynamic light scattering and analytical ultracentrifugation for the sizing of poly(butyl cyanoacrylate) nanoparticles. Eur. J. Pharm. Biopharm. 57, 369–375.

Boyd, B.J., Drummond, C.J., Krodkiewska, I., Grieser, F., 2000. How chain length, headgroup polymerization, and anomeric configuration govern the thermotropic and lyotropic liquid crystalline phase behavior and the air–water interfacial adsorption of glucose-based surfactants. Langmuir 16, 7359–7367.

Couvreur, P., Couarraze, G., Devissaguet, J., Puisieux, F., 1996. Nanoparticles: preparation and characterization. In: Benita, S. (Ed.), Microencapsulation: Methods and Industrial Applications. Marcel Dekker, New York, pp. 183–211.

Couvreur, P., Grislain, L., Lenaerts, V., Brasseur, F., Guiot, P., Biernacki, A., 1986. Biodegradable polymeric nanoparticles as drug carriers for antitumor agents. In: Guiot, P., Couvreur, P. (Eds.), Polymer Nanoparticles and Microspheres. CRC Press, Boca Raton, Florida, pp. 24–94.

Damge, C., Aprahamian, M., Balboni, G., Hoeltzel, A., Andrieu, V., Devissaguet, J.P., 1987. Polyalkylcyanoacrylate nanocapsules increase the intestinal-absorption of a lipophilic drug. Int. J. Pharm. 36, 121–125.

El-Samaligy, M.S., Rohdewald, P., Mahmoud, H.A., 1986. Polyalkyl cyanoacrylate nanocapsules. J. Pharm. Pharmacol. 38, 216–218.

Fiedler, H.P., 2002. Encyclopedia of excipients for pharmaceuticals, cosmetics and related areas, fifth ed. Editio Cantor Verlag, Aulendorf.

Fukuda, K., Olsson, U., Ueno, M., 2001. Microemulsion formed by alkyl polyglucoside and an alkyl glycerol ether with weakly charged films. Colloid Surf. B-Biointerfaces 20, 129–135.

Garti, N., Aserin, A., Ezrahi, S., Tiunova, I., Berkovic, G., 1996. Water behavior in nonionic surfactant systems. 1. Subzero temperature behavior of water in nonionic microemulsions studied by DSC. J. Colloid Interface Sci. 178, 60–68.

Garti, N., Aserin, A., Tiunova, I., Fanun, M., 2000. A DSC study of water behavior in water-in-oil microemulsions stabilized by sucrose esters and butanol. Colloid Surf. A-Physicochem. Eng. Asp. 170, 1–18.

Gasco, M.R., Trotta, M., 1986. Nanoparticles from microemulsions. Int. J. Pharm. 29, 267–268.

Ghi, P.Y., Hill, D.J.T., Whittaker, A.K., 2002. PFG-NMR measurements of the self-diffusion coefficients of water in equilibrium poly(HEMA-co-THFMA) hydrogels. Biomacromolecules 3, 554–559.

Gipps, E.M., Groscurth, P., Kreuter, J., Speiser, P.P., 1987. The effects of polyalkylcyanoacrylate nanoparticles on human normal and malignant mesenchymal cells in vitro. Int. J. Pharm. 40, 23–31.

Krauel, K., Davies, N.M., Hook, S., Rades, T., 2005. Using different structure types of microemulsions for the preparation of poly(alkylcyanoacrylate) nanoparticles by interfacial polymerization. J. Control. Release 106, 76–87.

Krauel, K., Graf, A., Hook, S.M., Davies, N.M., Rades, T., 2006. Preparation of poly(alkylcyanoacrylate) nanoparticles by polymerization of water-free microemulsions. J. Microencapsul. 23, 499–512.

Lherm, C., Muller, R.H., Puisieux, F., Couvreur, P., 1992. Alkylcyanoacrylate drug carriers. 2. Cytotoxicity of cyanoacrylate nanoparticles with different alkyl chain-length. Int. J. Pharm. 84, 13–22.

Lindman, B., Stilbs, P., 1987. Molecular diffusion in microemulsions. In: Friberg, S.E., Bothorel, P. (Eds.), Microemulsions: Structure and Dynamics. CRC Press, Boca Raton, Florida, pp. 119–152.

Lindman, B., Stilbs, P., Moseley, M.E., 1981. Fourier-transform NMR self-diffusion and microemulsion structure. J. Colloid Interface Sci. 83, 569–582.

Lowe, P.J., Temple, C.S., 1994. Calcitonin and insulin in isobutylcyanoacrylate nanocapsules—protection against proteases and effect on intestinal-absorption in rats. J. Pharm. Pharmacol. 46, 547–552.

McDowell, A., 2005. Oral delivery of bioactive compounds to the common brushtail possum (Trichosurus vulpecula). Ph.D thesis, University of Otago, Dunedin, New Zealand.

Moulik, S.P., Paul, B.K., 1998. Structure, dynamics and transport properties of microemulsions. Adv. Colloid Interface Sci. 78, 99–195.

Nilsson, P.G., Lindman, B., 1982. Solution structure of non-ionic surfactant micro-emulsions from nuclear magnetic-resonance self-diffusion studies. J. Phys. Chem. 86, 271–279.

Pitaksuteepong, T., Davies, N.M., Tucker, I.G., Rades, T., 2002. Factors influencing the entrapment of hydrophilic compounds in nanocapsules prepared by interfacial polymerisation of water-in-oil microemulsions. Eur. J. Pharm. Biopharm. 53, 335–342.

Saintruth, H., Attwood, D., Ktistis, G., Taylor, C.J., 1995. Phase studies and particle-size analysis of oil-in-water phospholipid microemulsions. Int. J. Pharm. 116, 253–261.

Sarciaux, J.M., Acar, L., Sado, P.A., 1995. Using microemulsion formulations for oral-drug delivery of therapeutic peptides. Int. J. Pharm. 120, 127–136.

Savic, S.D., Savic, M.M., Vesic, S.A., Vuleta, G.M., Muller-Goymann, C.C., 2006. Vehicles based on a sugar surfactant: colloidal structure and its impact on in vitro/in vivo hydrocortisone permeation. Int. J. Pharm. 320, 86–95.

Sharma, A., Kaur, R., Kumar, S., Gupta, P., Pandav, S., Patnaik, B., Gupta, A., 2003. Fibrin glue versus *N*-butyl-2-cyanoacrylate in corneal perforations. Ophthalmology 110, 291–298.

Singer, A.J., Zimmerman, T., Rooney, J., Cameau, P., Rudomen, G., McClain, S.A., 2004. Comparison of wound-bursting strengths and surface characteristics of FDA-approved tissue adhesives for skin closure. J. Adhes. Sci. Technol. 18, 19–27.

Trotta, M., Cavalli, R., Ugazio, E., Gasco, M.R., 1996. Phase behaviour of microemulsion systems containing lecithin and lysolecithin as surfactants. Int. J. Pharm. 143, 67–73.

Trotta, M., Gallarate, M., Pattarino, F., Carlotti, M.E., 1999. Investigation of the phase behaviour of systems containing lecithin and 2-acyl lysolecithin derivatives. Int. J. Pharm. 190, 83–89.

Trotta, M., Ugazio, E., Peira, E., Pulitano, C., 2003. Influence of ion pairing on topical delivery of retinoic acid from microemulsions. J. Control. Release 86, 315–321.

Vauthier, C., Dubernet, C., Fattal, E., Pinto-Alphandary, H., Couvreur, P., 2003. Poly(alkylcyanoacrylates) as biodegradable materials for biomedical applications. Adv. Drug Deliv. Rev. 55, 519–548.

von Rybinski, W., Hill, K., 1998. Alkyl Polyglycosides—properties and applications of a new class of surfactants. Angew. Chem. Int. Ed. Engl. 37, 1328–1345.

Watnasirichaikul, S., Davies, N.M., Rades, T., Tucker, I.G., 2000. Preparation of biodegradable insulin nanocapsules from biocompatible microemulsions. Pharm. Res. 17, 684–689.

Watnasirichaikul, S., Rades, T., Tucker, I.G., Davies, N.M., 2002a. Effects of formulation variables on characteristics of poly (ethylcyanoacrylate) nanocapsules prepared from w/o microemulsions. Int. J. Pharm. 235, 237–246.

Watnasirichaikul, S., Rades, T., Tucker, I.G., Davies, N.M., 2002b. In-vitro release and oral bioactivity of insulin in diabetic rats using nanocapsules dispersed in biocompatible microemulsion. J. Pharm. Pharmacol. 54, 473–480.